Remote Sensing of Environment 138 (2013) 19–26

Contents lists available at ScienceDirect

Remote Sensing of Environment

journal homepage: www.elsevier.com/locate/rse

Monitoring and analysis of grassland desertification dynamics using Landsat images in Ningxia, China

Jinya Li [a], Xiuchun Yang [a], Yunxiang Jin [a], Zhi Yang [b], Wenguang Huang [c], Lina Zhao [d], Tian Gao [a], Haida Yu [a], Hailong Ma [a], Zhihao Qin [a], Bin Xu [a,*]

[a] Key Laboratory of Agri-informatics of the Ministry of Agriculture, Institute of Agricultural Resources and Regional Planning, Chinese Academy of Agricultural Sciences, Beijing 100081, China
[b] Grassland Monitoring and Supervision Center of the Ministry of Agriculture, Beijing 100125, China
[c] Ningxia Grassland Monitoring and Supervision Center, Yinchuan 750002, China
[d] Institute of Botany, Chinese Academy of Sciences, Beijing 100093, China

ARTICLE INFO

Article history:
Received 19 March 2013
Received in revised form 1 July 2013
Accepted 2 July 2013
Available online 10 August 2013

Keywords:
Grassland desertification
Spectral mixture analysis
Spatiotemporal analysis
Grazing ban
Ningxia

ABSTRACT

State and local governments in China have implemented a series of grassland protection policies to address the problem of grassland degradation. In 2003, Ningxia was the first province to implement a province-wide grazing ban. The effect of this ban is contentious at all levels of government and has become a topic of public concern. Grassland desertification is the most direct indicator of the effect of the grazing ban. We selected 14 counties and cities in north-central Ningxia as the study area. A desertification classification and grading system for Ningxia's grassland was then designed based on fieldwork and expert review. Using the Spectral Mixture Analysis (SMA) and decision-tree methods, we interpreted Landsat TM/ETM+ images of the study area during four years: 1993, 2000, 2006 and 2011. The following results were obtained: from 1993 to 2011, the area of desertified grassland in north-central Ningxia decreased gradually from 8702 km^2 in 1993 to 7485 km^2 in 2011, a decrease of 13.98%; the degree of desertification gradually decreased from 3573 km^2 of severely desertified grassland in 1993 to 1450 km^2 in 2011, a decrease of 59.41%; desertified grassland vegetation was restored rapidly during 2000–2006 and 2006–2011, reducing the total area of desertified grassland annually by 1.87 and 0.61%, respectively; finally, the area of severely desertified grassland decreased annually by 5.78 and 6.28% during 2000–2006 and 2006–2011, respectively. These results show that the region-wide grazing ban, together with other ecological engineering measures, has helped reverse desertification and promote the restoration of grassland vegetation.

1. Introduction

Grassland desertification, the primary form of grassland degradation, is defined as the degradation of grasslands in arid, semi-arid and dry sub-humid areas. Non-desert grasslands in these areas typically include aeolian sand, similar to desert landscapes, and desertified grasslands (DGs) are grasslands where the action of sand is further exacerbated due to climate variation and/or human activity. China has nearly 400 million ha of natural grasslands, representing 41.7% of its territory. However, 90% of China's available natural grasslands exhibit varying degrees of degradation, half of which is manifested as reduced vegetative coverage, desertification, salinization, and other characteristics of moderate or severe degradation (Development Planning Department of Agriculture, 2002). In the face of increasingly serious grassland desertification, accurate, timely and effective monitoring of grassland desertification is essential to understanding the grassland desertification process and to establishing early warning measures for the prevention of desertification (Reynolds et al., 2007). Because a field measurement is expensive, labor-intensive and often limited with regard to its temporal and spatial scale, remote-sensing data (which yield multi-temporal data covering a wide spatial extent that are periodically repeated) allow for the monitoring of changes in grassland desertification (Rogan, Franklin, & Roberts, 2002; Yang & Liu, 2005).

The Ningxia Hui Autonomous Region, which has a total area of 51,800 km^2, is located primarily in arid and semi-arid zones and is surrounded by the Tengger Desert, the Ulan Buh Desert and the Mu Us Sandland in the west, north and east, respectively. This region is also one of the most desertified provinces in China. Some studies have indicated that the desertified area in Ningxia has been significantly reduced due to the implementation of the Three-North Shelterbelt Forest Program, the Grain for Green Project and the region-wide grazing ban, among other ecological engineering measures. These measures were implemented over the last few years after Ningxia was chosen as a sand prevention and control demonstration region. These studies also indicate that the desertification process has been reversed, showing that the sand prevention and control work has achieved significant results (Huang et al., 2011; Yan, Wang, Feng, & Wang, 2003; Yang,

* Corresponding author. Tel.: +86 13910571556.
E-mail address: xubin@caas.cn (B. Xu).

0034-4257/$ – see front matter © 2013 Elsevier Inc. All rights reserved.
http://dx.doi.org/10.1016/j.rse.2013.07.010

Wu, & Shen, 2013). However, other studies have indicated that the harsh natural environment and underdeveloped economic conditions in Ningxia have caused the ecology of the sandy area to become extremely fragile. The trend of desertification, officially described as "overall reversal but partial deterioration," still exists. Further development of the anti-desertification work and stabilization of the desertification reversal zone, among other measures, remain necessary (Yu, Wang, Jiang, Ren, & Li, 2011). Currently, little monitoring of Ningxia's desertification is conducted. Most of the monitoring consists of ground-survey methods, which are time-consuming and limited in their assessment of the overall spatial distribution and trend of desertification in Ningxia; other monitoring efforts involve the visual interpretation of remote-sensing images to determine the extent of Ningxia's desertification (Jia & Zhang, 2011), a process that is more subjective.

In the present study, we selected 14 counties and cities in the north-central part of Ningxia as the study area. A Ningxia grassland desertification classification and grading system was constructed based on Landsat TM/ETM+ remote-sensing images, field observations and expert review, and remote-sensing interpretation symbols representing different grassland desertification levels were established. Spectral Mixture Analysis (SMA) and decision-tree methods were then selected to interpret the data from the four periods (1993, 2000, 2006 and 2011).

2. Materials and methods

2.1. Study area

The Ningxia Hui Autonomous Region is located at 104°17′E–107°39′E, 35°14′N–39°23′N along the upper reaches of the Yellow River. The region is approximately 456 km long from north to south and 250 km wide from east to west. The entire territory from north to south is divided into six geomorphic regions: the Helan Mountains, the Yinchuan Plain, the Lingyan Mesa, the mountainous region and inter-mountainous plain, the loess hills and the Liupanshan mountains. The annual precipitation in the region ranges from 180 to 350 mm, the annual evaporation ranges from 2100 to 2300 mm, and the region has an aridity of 3.3 to 4.7 (Guo, Xin, & Cao, 1995).

The study area, located in north-central Ningxia, includes 14 administrative counties and cities (Fig. 1), which cover 67.5% of the total area of Ningxia. The study area includes the following three main desert zones: the Mu Us sandy land area, the Tengger sandy area and the Yellow River Plain sandy irrigation area.

2.2. Data acquisition and pre-processing

Landsat TM/ETM+ scenes obtained in 1993, 2000 and 2006 were selected because they have similar precipitation and high data quality. The TM images acquired in 2011 were selected to interpret the recent grassland desertification status, whereas the former three years were used to analyze the effect before and after the implementation of the region-wide grazing ban in 2003. These time-series Landsat images, with a spatial resolution of 30 m, were obtained during summer and autumn (July–August), when vegetation typically reaches its maximum growth during the region's growing season. The images were downloaded from the United States Geological Survey (USGS) (http://glovis.usgs.gov) at no cost or were purchased from the Center for Earth Observation and Digital Earth (CEODE) at the Chinese Academy of Sciences. In addition, we purchased one Spot-5 HRVIR image (September 13, 2011) with spatial resolutions of 2.5 m (panchromatic band) and 10 m (multi-spectral band) covering the central part of the study area, which aided in the establishment of Landsat TM/ETM+ interpretation keys. Geometric correction (to reduce the error to less than 0.5 pixels), atmospheric correction and other image processing were performed for the 12-scene Landsat TM/ETM+ images. Ortho-rectification, geometric correction, true-color conversion and band fusion (positioning accuracy after fusion at 5 m) were performed for the Spot-5 HRVIR images.

The basic study-area data, including the annual land-use map, the meteorological data (rainfall, temperature, etc.), the grassland-type map and the soil-type map, were collected and collated.

2.3. Grassland desertification evaluation system and indicators

In the 1980s, the Food and Agriculture Organization (FAO) and the United Nations Environment Programme (UNEP) developed a provisional methodology for the assessment and mapping of desertification. The methodology consists of 22 indicators, many of which can only be obtained from field measurements, which are difficult to obtain, and from a wide range of monitoring techniques that are even more difficult (Symeonakis & Drake, 2004). Formulating a system of universal grassland desertification monitoring indicators is a challenging task (Sommer et al., 2011) due to the regional differences in the type of grassland desertification, the evaluation criteria and the conceptual understanding of grassland desertification. However, because grassland desertification monitoring is based on specific aspects of the study area, the interpretation of grassland desertification indicators is simplified as

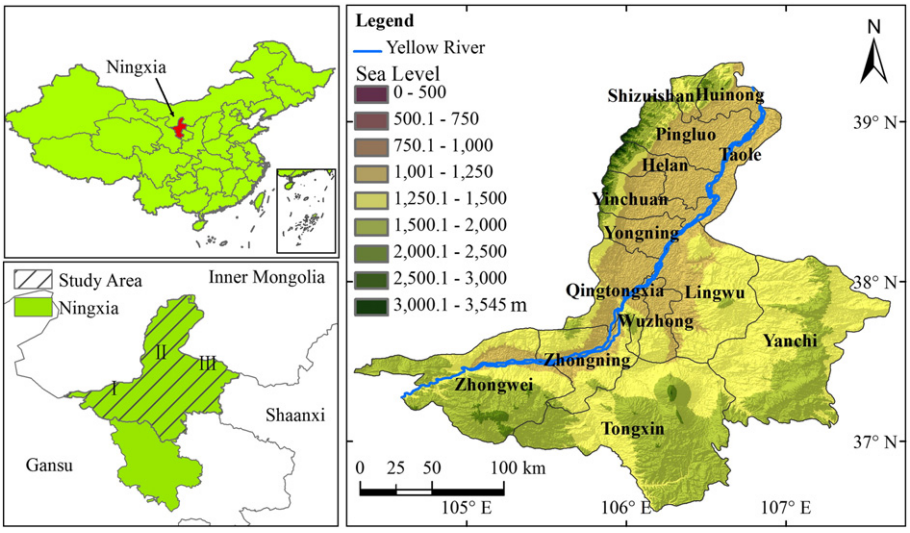

Fig. 1. Location of the Ningxia Hui Autonomous Region and the study area. I is the Tengger sandy area, II is the Yellow River Plain sandy irrigation area, and III is the Mu Us sandy land area.

Table 1
Remote sensing gradation system of grassland desertification in Ningxia. The bare-sand ratio represents the percentage cover of sandy soil in each plot.

Grassland desertification intensity classification	Vegetation community characteristics		Bare-sand ratio(%)	Geo-morphological features
	Vegetation composition	Vegetation coverage(%)		
SlDG	Psammophytes become the main accompanying species.	40–55	30–50	Relatively moderate sand, fixed sand dunes.
MDG	Psammophytes become the dominant species.	30–40	50–65	Moderate sand, small blowout pits or semi-fixed sand dunes.
SeDG	Vegetation is sparse, only a few psammophytes remaining.	<30	>65	Medium and large sand dunes, large blowout pits, semi-mobile or mobile sand dunes.

major factors are highlighted and less attention is paid to secondary information. This simplification results in improved and more easily undertaken grassland desertification monitoring (Symeonakis & Drake, 2004; Zucca, Peruta, Salvia, Sommer, & Cherlet, 2012). Subsequent grassland desertification research based on field observations has also shown that one or more indicators are dominant (Boer & Puigdefabregas, 2005; Del Barrio, Puigdefabregas, Sanjuan, Stellmes, & Ruiz, 2010; Evans & Geerken, 2004; Helldén & Tottrup, 2008; Sharma, 1998; Wessels, Prince, & Reshef, 2008).

We classified the land-cover type of the study area into nine categories: farmland, forest, human settlements, water, non-desertified grassland (non-DG), slightly desertified grassland (SlDG), moderately desertified grassland (MDG), severely desertified grassland (SeDG) and others. These categories were based on China's desertification classification indicator studies (Ding, Zhao, Fan, & Du, 2004; Dong & Liu, 1992; Gao, Wang, Zhu, Wang, & Zhang, 1998; Li et al., 2011; Wang & Sun, 1996; Wang et al., 2004) and China's national standard "parameters for degradation, sandification and salification of rangelands" (GB19377-2003). Furthermore, we incorporated field inspection and verification combined with land-use characteristics to establish the basic desertification characteristics and the grassland type of the study area. Finally, we conducted seminars and demonstration projects with experts to substantiate the scientific validity, operability and interpretability of the remote-sensing images. Combining the sample plots and quadrat data, the grassland type and environment of the study area, we further refined the remote sensing gradation system of grassland desertification in Ningxia (Table 1).

2.4. Grassland desertification information extraction method

The NDVI (Normalized Difference Vegetation Index) and other vegetation information-based methods used to indirectly monitor grassland desertification often tend to overestimate the degree of desertification in sparsely vegetated areas due to the instability of seasonal vegetation changes, the severe effect of rainfall and other factors (Dawelbait & Morari, 2010; Li, 2011; Wessels, van den Bergh, & Scholes, 2012). Furthermore, it is difficult to establish a direct relationship between grassland desertification and vegetation coverage. Therefore, based on long-term desertification evaluation experiments, we selected the bare-sand ratio and vegetation coverage as the main bases for evaluating grassland desertification, and we used SMA as the primary method for extracting the bare-sand ratio and vegetation coverage. The Linear Spectral Mixture Model (LSMM), one type of SMA, is widely used due to its simplicity, reasonable level of effectiveness and interpretability (Collado, Chuvieco, & Camarasa, 2002; Dawelbait & Morari, 2012; Elmore, Mustard, Manning, & Lobell, 2000; Yang, Weisberg, & Bristow, 2012). In an LSMM, the reflectance of each pixel at each spectral band is presented as a linear combination of the reflectance of each endmember and its relative abundance (Ichoku & Karnieli, 1996) as follows:

$$\rho(\lambda_i) = \sum_{j=1}^{m} F_j \rho_j(\lambda_i) + \varepsilon(\lambda_i) \quad (1)$$

where $j = 1, 2, \ldots m$ is the pixel component (endmember); $i = 1, 2, \ldots n$ is the spectral band, $m \le n + 1$; $\rho(\lambda_i)$ is the reflectance of mixed pixels for each band (i); $\rho_j(\lambda_i)$ is the reflectance of endmember j at band i; F_j is the abundance of endmember j in the pixel (a parameter to be estimated); and $\varepsilon(\lambda_i)$ is the difference between the actual and modeled reflectance. F_j represents the best fit coefficient that minimizes the *RMS* error given by the following equation:

$$RMS = \sqrt{\left(\sum_{i=1}^{n} \varepsilon^2(\lambda_i)\right) \Big/ n} \quad (2)$$

where n is the number of bands and $\varepsilon(\lambda_i)$ is the residual term at band i ($i = 1, 2, \ldots n$).

The derived fractions of endmembers are often subject to the unity constraint, which is derived as follows:

$$\sum_{j=1}^{m} F_j = 1. \quad (3)$$

Appropriate and accurate endmember selection is crucial for the success of the LSMM (Elmore et al., 2000; Tompkins, Mustard, Pieters, & Forsyth, 1997). The selection process involves identifying both the number and type of endmembers and their corresponding spectral signatures (Somers, Asner, Tits, & Coppin, 2011). The following criteria are most frequently used: (1) the *RMS* should be as small as possible, (2) $0 \le F \le 1$ and (3) the endmember should be representative and should be an effective component of most of the images within the pixel. The *RMS* should not be blindly pursued but should take full account of the validity and accuracy of the spectral unmixing model, which requires constant comparison and verification with field sampling data. In the present study, a comprehensive field investigation was conducted to identify the optimal/most representative surface types and to find suitable locations for developing a spectral library from the image. Based on a field investigation, the TM/ETM+ images were processed using a Minimum Noise Fraction (MNF) rotation

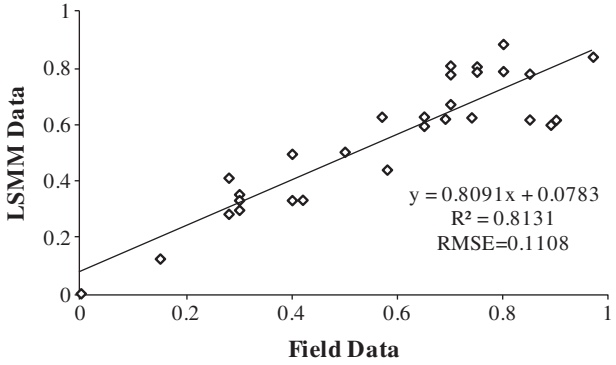

Fig. 2. Scatter plot correlation between the field-measured and LSMM-estimated bare-sand fraction in 2011. The linear relationships for the validation are statistically significant at $P < 0.0001$.

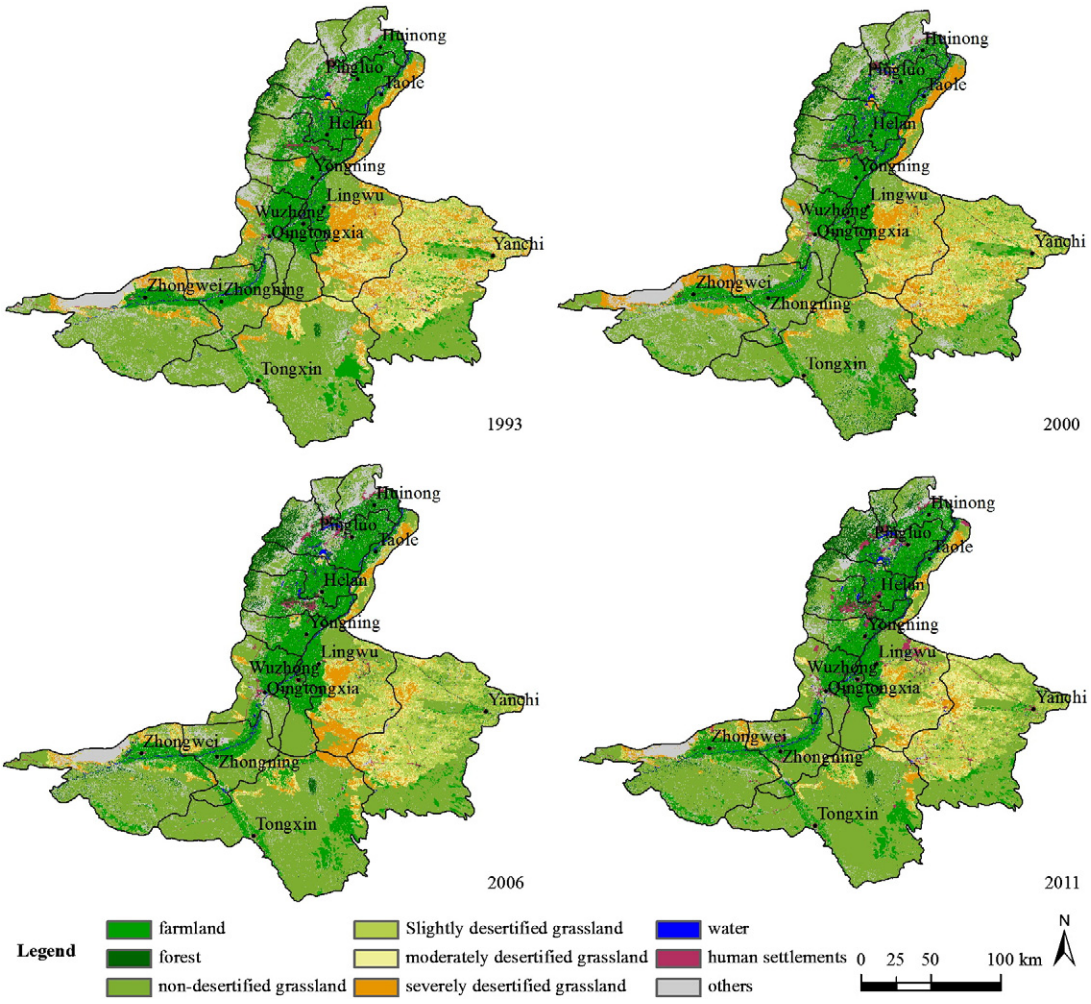

Fig. 3. Grassland desertification monitoring results in north-central Ningxia (the study area) during four periods.

transformation; thus, the "pure" spectral endmembers of vegetation, bare sand and bare soil were extracted by iteratively testing different endmember combinations (Franke, Roberts, Halligan, & Menz, 2009; Garc I A-Haro, Sommer, & Kemper, 2005; Ghrefat & Goodell, 2011). These endmembers were then input into the spectral unmixing algorithm, thereby producing a bare-sand fraction map and a vegetation coverage map.

Before producing unmixed pixels, a mask was made for farmland, human settlements, water, forest and other land uses based on visual interpretation, the NDWI (Normalized Difference Water Index) and the NDVI, among other methods. The distribution of grassland desertification was determined by applying a visual interpretation method to the masked images, and the result was then input into the LSMM.

2.5. Validation

A two-week field survey was conducted to establish a grassland desertification classification system suitable for the study area and to evaluate the accuracy of the LSMM using the ground bare-sand ratio and vegetation coverage data as a reference. A total of 41 plots were

Table 2
Area and proportion of each major class during various periods in the study area (area: km^2; proportion: %).

Land type	1993		2000		2006		2011	
	Area	Proportion	Area	Proportion	Area	Proportion	Area	Proportion
SlDG	1817	5.2	3042	8.7	3604	10.31	3762	10.76
MDG	3312	9.48	2414	6.91	2002	5.73	2273	6.5
SeDG	3573	10.22	3237	9.26	2114	6.05	1450	4.15
Total DG	8702	24.9	8694	24.87	7720	22.09	7485	21.42
Non-DG	15,214	43.53	14,449	41.34	15,467	44.25	16,176	46.28
Farmland	5388	15.42	5829	16.68	6172	17.66	6033	17.26
Forest	829	2.37	1266	3.62	1530	4.38	1662	4.75
Water	234	0.67	265	0.76	284	0.81	313	0.89
Human settlements	317	0.91	341	0.97	407	1.16	826	2.36
Other	4267	12.21	4107	11.75	3371	9.65	2456	7.03

Table 3
Annual change rate of each class during various periods in the study area (positive values represent an increase; negative values represent a decrease; unit: %).

Period	SlDG	MDG	SeDG	Total DG	Non-DG	Farmland	Forest	Water	Human settlements	Other
1993–2000	9.64	−3.87	−1.34	−0.01	−0.72	1.17	7.51	1.9	1.08	−0.54
2000–2006	3.07	−2.84	−5.78	−1.87	1.17	0.98	3.48	1.22	3.25	−2.98
2006–2011	0.88	2.71	−6.28	−0.61	0.92	−0.45	1.73	2.01	20.6	−5.43
1993–2011	5.95	−1.74	−3.3	−0.78	0.35	0.66	5.57	1.88	8.93	−2.36

selected. After excluding the plots used for endmember selection, 29 plots were left for validation. The accuracy of the LSMM was estimated by scatter plot correlation comparing the bare-sand ratio in each plot with the bare sand fraction image in 2011 (Fig. 2). The validation results for the three historical periods 1993, 2000 and 2006 were estimated by comparing the final classification results with the visual interpretation results in the 50 pixels, which were randomly selected from the images separately.

3. Results

3.1. Grassland desertification time variation characteristics

3.1.1. Grassland desertification change characteristics during different periods

The results obtained for the four periods during which Ningxia's grassland desertification was monitored are shown in Fig. 3, and the resultant data are shown in Table 2. By combining the classification maps from the four periods and statistical results from 1993 to 2011, we obtained a total area for the three levels of desertified grassland in 1993 of 8702 km^2. Based on the monitoring results obtained for 2000, 2006 and 2011, the area of desertified grassland decreased gradually to 7485 km^2 in 2011 (at the end of monitoring period), which represents a decrease of 13.98%; from 2000 to 2006, the area of desertified grassland was reduced by 974 km^2, representing a decrease of 11.20%. This significant decrease may have an important correlation with the region-wide grazing ban in Ningxia that began in 2003. The SeDG area decreased from 3573 km^2 in 1993 to 1450 km^2 in 2011, a decrease of 59.41%. From 2000 to 2006, the SeDG area decreased by 34.70%, and the restoration of grassland vegetation was significant. The MDG area exhibited a decreasing trend; however, this area increased steadily after 2006. The SlDG area increased from 1817 km^2 in 1993 to 3762 km^2 in 2011, an increase of 107.07%.

The gradual decrease in the extent of the SeDG area, the rapid increase in the SlDG area and the decrease in total DG area indicate that grassland desertification in Ningxia has reversed during the past two decades. The vegetation is in a state of recovery, and the grassland environment has achieved marked improvement, especially after the 2003 region-wide grazing ban was implemented.

3.1.2. Annual rate of grassland desertification change during various periods

An annual gradient was obtained by further processing grassland desertification and other land-type data from various periods (Table 3).

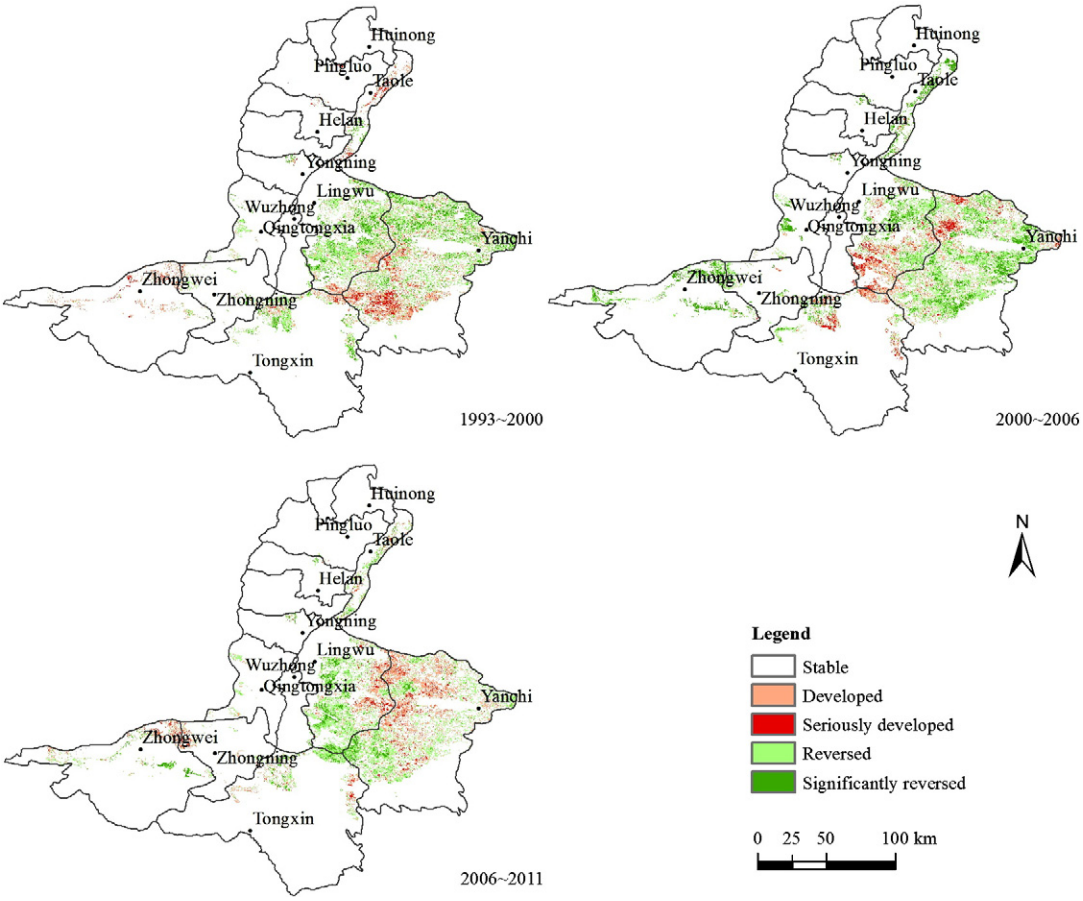

Fig. 4. Grassland desertification spatial distribution dynamic-change maps for north-central Ningxia.

Table 4
Transfer matrix of grassland desertification change for the study area from 1993 to 2000 (unit:km^2).

2000	1993								
	SlDG	MDG	SeDG	Non-DG	Farmland	Forest	Water	Human settlements	Other
SlDG	915	1253	637	42	111	1	1	0	82
MDG	491	1047	733	22	39	1	0	0	80
SeDG	248	798	1915	15	21	1	0	0	239
Non-DG	107	113	101	11,997	495	78	37	1	1520
Farmland	30	51	66	890	4168	388	53	7	177
Forest	5	3	3	394	339	306	18	66	131
Water	1	0	1	54	52	12	95	8	41
Human settlements	4	10	8	23	35	12	1	233	15
Other	16	37	109	1776	128	30	29	1	1981

These data show that the annual change in SlDG for three different periods was 9.64, 3.07 and 0.88%. The fastest growth occurred before 2000, and the rate gradually decreased thereafter. The annual MDG reduction rate was 3.87% from 1993 to 2000 and 2.84% from 2000 to 2006; it then began to increase annually by 1.98%. SeDG showed a decreasing trend in all three periods, and the rate of decrease gradually accelerated. The annual rate of decrease was 1.34% before 2000 but was higher during both periods after 2000 (the annual reduction rate of SeDG from 2000 to 2006 and from 2006 to 2011 was 5.78 and 6.28%, respectively), suggesting that the 2003 region-wide grazing ban and other ecological engineering measures played important roles in the rapid recovery of the DG vegetation and the reversal of the overall trend of grassland desertification.

3.2. Grassland desertification spatial variation characteristics

Using raster calculations, as implemented in ArcGIS, we constructed grassland desertification spatial distribution dynamic change maps (Fig. 4) for 1993–2000, 2000–2006 and 2006–2011. We define the figure elements as follows: an increase in the degree of desertification from the previous period indicates "developed" (e.g., a change from non-DG to SlDG); a cross-level increase indicates "seriously developed" (e.g., a change from non-DG to MDG); a decrease indicates "reversed"; a cross-level decrease indicates "significantly reversed"; and no change between two periods indicates "stable" (Li et al., 2011). We obtained a transfer matrix for each period in the study area using the Change Detection Statistics function of ENVI.

From 1993 to 2000, 491 and 248 km^2 of SlDG changed into MDG and SeDG, respectively, and 1253 and 798 km^2 of MDG changed into SlDG and SeDG, respectively. At the same time, 637 and 733 km^2 of SeDG changed into SlDG and MDG, respectively. The non-DG area that changed into slightly, moderately and severely DG was small (42, 22 and 15 km^2, respectively (Table 4)).

From 1993 to 2000, 2944 km^2 of DG was either reversed or significantly reversed and was mainly distributed in northern Yanchi County and central Lingwu County. At the same time, 1618 km^2 of the grassland was developed, significantly developed or converted into DG from other land types; this area was mainly distributed in southern Yanchi County. The total area of reversed and significantly reversed DG was 1.82 times that of developed and significantly developed DG, indicating that, overall, the DG in the study area was in a state of recovery or reversal (Fig. 4).

From 2000 to 2006, 479, 262 and 557 km^2 of SlDG changed to MDG, SeDG and non-DG, respectively, with a larger proportion changing to non-DG. A total of 488 km^2 of MDG changed to SeDG, and 1011 km^2 of MDG changed to SlDG (2.07 times the area that changed to SeDG). In addition, 804 and 826 km^2 changed to slightly and moderately DG from SeDG, respectively (slightly greater than the total area changed during the previous period (Table 5)).

From 2000 to 2006, 3599 km^2 of DG was reversed or significantly reversed and was mainly distributed in central Yanchi County and in northern Lingwu County. A total of 1417 km^2 of DG was developed, significantly developed or converted into DG from another land type (mainly distributed in northwestern Yanchi County and southern Lingwu County) (Fig. 4). The area of DG vegetation restoration expanded and the developed area narrowed, showing that the implementation of the region-wide grazing ban in 2003, which Ningxia was the first province/autonomous region in the country to implement, has effectively promoted sand zone vegetation recovery.

From 2006 to 2011, 777, 186 and 515 km^2 of SlDG changed to MDG, SeDG and non-DG, respectively; 351 km^2 of MDG changed to SeDG; and 824 km^2 of MDG changed to SlDG, 2.35 times the change to SeDG. Areas of 403 and 721 km^2 changed from SeDG to slightly and moderately DG, respectively, slightly less than the area converted during the previous period (Table 6).

From 2006 to 2011, 2578 km^2 of DG was reversed or significantly reversed and was mainly distributed in central Lingwu County and in southwestern Yanchi County; 1733 km^2 of DG was developed, significantly developed or converted to DG from other land types and was mainly distributed in the north of Yanchi County and in the east of Lingwu County (Fig. 4). The area of desertification development and significant development was smaller than the area of reversal and significant reversal, showing that grassland was still recovering from desertification in the study area.

Table 5
Transfer matrix of grassland desertification change in the study area from 2000 to 2006 (unit: km^2).

2006	2000								
	SlDG	MDG	SeDG	Non-DG	Farmland	Forest	Water	Human settlements	Other
SlDG	1550	1011	804	146	53	2	1	0	38
MDG	479	615	826	31	12	0	0	0	39
SeDG	262	488	1263	10	6	0	0	0	84
Non-DG	557	210	191	11,938	537	290	10	1	1733
Farmland	81	44	60	638	4972	200	37	8	131
Forest	11	3	4	421	110	570	60	80	270
Water	2	1	3	61	23	29	120	3	43
Human settlements	4	5	6	30	22	49	6	248	38
Other	96	36	81	1175	94	126	31	1	1731

Table 6
Transfer matrix of grassland desertification change in the study area from 2006 to 2011 (unit: km^2).

2011	2006								
	SlDG	MDG	SeDG	Non-DG	Farmland	Forest	Water	Human settlements	Other
SlDG	2006	824	403	353	103	3	0	0	69
MDG	777	687	721	58	7	1	0	0	22
SeDG	186	351	861	8	3	0	0	0	42
Non-DG	515	75	40	13,557	566	184	13	1	1225
Farmland	36	14	13	474	4842	367	49	25	213
Forest	5	2	2	130	394	705	36	30	357
Water	2	2	2	15	57	30	170	2	32
Human settlements	34	27	30	149	58	99	4	347	79
Other	42	22	42	722	142	140	13	1	1332

4. Discussion

To improve the comparability between periods, this paper attempted to select remote sensing data for years with similar precipitation. Using the LSMM and decision-tree methods, among other approaches, this paper interpreted remote-sensing images representing four periods over nearly two decades and analyzed the spatial and temporal variations of grassland desertification in Ningxia before and after the implementation of the grazing ban program to more accurately illustrate the effect of the ban and historical changes in Ningxia grassland desertification.

The results obtained show that the grassland desertification in the north-central part of Ningxia is mainly distributed in Yanchi County, Lingwu County and Taole County. From 1993 to 2011, the DG area in the north-central part of Ningxia experienced an overall gradual decreasing trend from 8702 km^2 in 1993 to 7485 km^2 in 2011, representing a decrease of 13.98%, with a net reversal of 1216 km^2 of DG to non-DG. Of the three DG classes, the SlDG area continuously increased, whereas that of MDG decreased at first but then increased steadily after 2006. SeDG decreased continuously from 3573 km^2 in 1993 to 1450 km^2 in 2011, representing a decrease of 59.41% and an annual decrease of 3.30%. From 2000 to 2006, the SeDG area decreased by 1123 km^2, representing 52.93% of the total decreased area and an annual decrease of up to 5.78%. Before the implementation of the grazing ban, the annual decrease in SeDG was only 1.34% from 1993 to 2000, showing the significant effect of the grazing ban on grassland desertification control.

Grassland desertification is the result of a combination of natural and human factors. Vegetation growth is closely linked to climatic factors (such as precipitation and temperature). Because Ningxia is in the transition zone between semi-arid and arid zones, the region is more highly influenced by precipitation. This study shows that during the monitoring period, Ningxia experienced an overall warming and drying trend. The average temperature trended upward, and the overall average annual precipitation trended downward (Fig. 5). The rainfall decreased significantly during the summer and autumn seasons (Wan & Yan, 2012; Xu, Tang, Du, & Bao, 2012). Ningxia's climate is changing in a direction that is not conducive to the restoration of grassland vegetation and desertification reversal. However, the results obtained here demonstrate that Ningxia's grassland vegetation has continually been restored and that there has been a gradual decrease in the degree of desertification and in the extent of the desertified area, indicating that human effort can effectively contribute to the reversal of desertification. Since Ningxia implemented the Grain for Green Project in 2000, the Three-North Shelterbelt Forest Program and, in particular, the region-wide grazing ban in 2003, the grassland vegetation has recovered more rapidly, and grassland desertification has been effectively controlled. This finding further shows that the implementation of grazing bans or of moderate grazing in arid and semi-arid sandy grasslands are effective measures to restore vegetation and prevent grassland desertification.

5. Conclusions

With the increasing complexity of human impacts on the environment, in the number of stressors and in the importance of cumulative impacts, monitoring and accurate assessment of the status and variation trends of grassland desertification are instrumental to developing efficient environmental management strategies (Rubio & Bochet, 1998). Using satellite- and field-observation-based data, the present study revealed a change in the overall degree and area of grassland desertification in north-central Ningxia, China, before and after the implementation of a series of ecological engineering measures, particularly the region-wide grazing ban that was first implemented in this region. In the context of this study, we wish to emphasize the importance of national and provincial ecological engineering measures that can be used to effectively combat desertification, despite the negative effects of climate change.

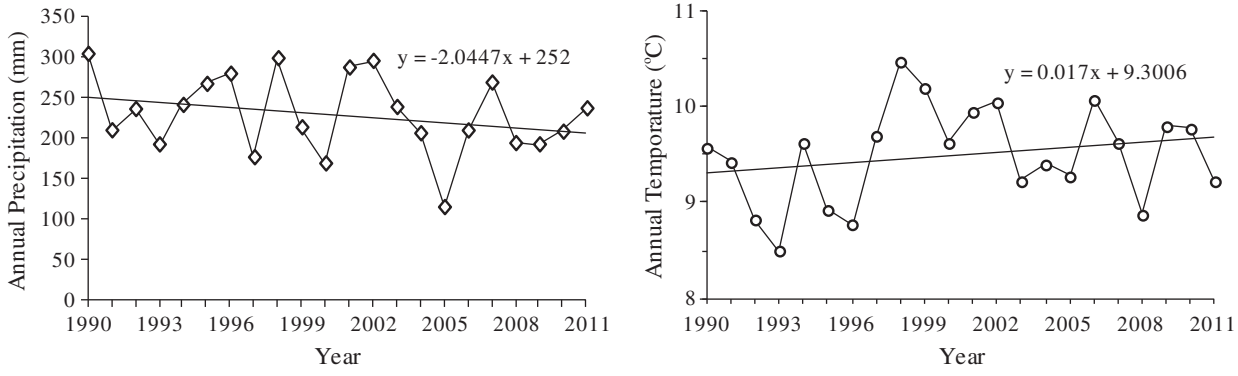

Fig. 5. Change in annual precipitation and temperature in the study area from 1990 to 2011. The annual precipitation and temperature were calculated using the weather data of Taole, Zhongning, Yanchi and Tongxin Counties. A more detailed analysis of the characteristics of climate change in Ningxia can be found in the studies by Wan and Yan (2012) and Xu et al. (2012).

This study demonstrates that satellite data, especially Landsat data, are useful for the long-term retrospective monitoring of environmental change. However, despite our promising results, there are limitations to the accuracy of desertification monitoring using Landsat data, and high-resolution tools must be applied. In this study, the application of SMA to Landsat data appeared to be a consistent, accurate and low-cost technique for obtaining objective information on the vegetation coverage and the bare-sand ratio of the region studied.

Acknowledgments

We are grateful for the strong support and guidance received during this research project from a number of leaders at the Grassland Supervisory Center of the Ministry of Agriculture and for the support and help given by the Grassland Supervisory Center of the Ningxia Hui Autonomous Region and by the grassland workstations of various cities and counties in the study area during our fieldwork.

References

Boer, M. M., & Puigdefabregas, J. (2005). Assessment of dryland condition using spatial anomalies of vegetation index values. *International Journal of Remote Sensing*, *26*, 4045–4065.

Collado, A.D., Chuvieco, E., & Camarasa, A. (2002). Satellite remote sensing analysis to monitor desertification processes in the crop-rangeland boundary of Argentina. *Journal of Arid Environments*, *52*, 121–133.

Dawelbait, M., & Morari, F. (2010). Limits and potentialities of studying dryland vegetation using the optical remote sensing. *Italian Journal of Agronomy*, *3*, 97–106.

Dawelbait, M., & Morari, F. (2012). Monitoring desertification in a Savannah region in Sudan using Landsat images and spectral mixture analysis. *Journal of Arid Environments*, *80*, 45–55.

Del Barrio, G., Puigdefabregas, J., Sanjuan, M. E., Stellmes, M., & Ruiz, A. (2010). Assessment and monitoring of land condition in the Iberian Peninsula, 1989–2000. *Remote Sensing of Environment*, *114*, 1817–1832.

Development Planning Department of Agriculture (2002). *National Grassland Ecological Construction Planning*. Beijing: Agriculture Press.

Ding, G. D., Zhao, Y. N., Fan, J. Y., & Du, H. (2004). Analysis on development of desertification assessment indicator system. *Journal of Beijing Forestry University*, *26*, 92–96.

Dong, Y. X., & Liu, Y. H. (1992). Study on the criteria system for desertification monitoring. *Arid Environmental Monitoring*, *6*, 179–182.

Elmore, A. J., Mustard, J. F., Manning, S. J., & Lobell, D. B. (2000). Quantifying vegetation change in semiarid environments: Precision and accuracy of spectral mixture analysis and the normalized difference vegetation index. *Remote Sensing of Environment*, *73*, 87–102.

Evans, J., & Geerken, R. (2004). Discrimination between climate and human-induced dryland degradation. *Journal of Arid Environments*, *57*, 535–554.

Franke, J., Roberts, D. A., Halligan, K., & Menz, G. (2009). Hierarchical multiple endmember spectral mixture analysis (MESMA) of hyperspectral imagery for urban environments. *Remote Sensing of Environment*, *113*, 1712–1723.

Gao, S. W., Wang, B. F., Zhu, L. Y., Wang, J. H., & Zhang, Y. G. (1998). Monitoring and evaluation indicator system on sandy desertification of China. *Scientia Silvae Sinicae*, *34*, 1–10.

Garc I A-Haro, F. J., Sommer, S., & Kemper, T. (2005). A new tool for variable multiple endmember spectral mixture analysis (VMESMA). *International Journal of Remote Sensing*, *26*, 2135–2162.

Ghrefat, H. A., & Goodell, P. C. (2011). Land cover mapping at Alkali Flat and Lake Lucero, White Sands, New Mexico, USA using multi-temporal and multi-spectral remote sensing data. *International Journal of Applied Earth Observation and Geoinformation*, *13*, 616–625.

Guo, S. J., Xin, Z. Z., & Cao, H. G. (1995). Sandification and countermeasures of grassland in Ningxia. *Journal of Arid Land Resources and Environment*, *9*, 70–73.

Helldén, U., & Tottrup, C. (2008). Regional desertification: A global synthesis. *Global And Planetary Change*, *64*, 169–176.

Huang, W. G., Liu, X. D., Yu, Z., Ma, X. M., Ma, Z., & Wang, L. (2011). Effects of grazing prohibition on grassland coverage — a case study at Yanchi County of Ningxia. *Pratacultural Science*, *28*, 1502–1506.

Ichoku, C., & Karnieli, A. (1996). A review of mixture modeling techniques for sub-pixel land cover estimation. *Remote Sensing Reviews*, *13*, 161–186.

Jia, K. L., & Zhang, J. H. (2011). Analysis of spatial–temporal changes of land use in ecologically vulnerable area — a case study in arid regions of central Ningxia. *Agricultural Research in the Arid Areas*, *29*, 221–225.

Li, J. Y. (2011). The research and application of methods used in grassland sandy desertification monitoring based on TM data. *Chinese Academy of Agricultural Sciences*.

Li, J. Y., Xu, B., Yang, X. C., Jin, Y. X., Li, Y. Y., Zhang, J., et al. (2011). Dynamic changes and driving force of grassland sandy desertification in Xilin Gol. A case study of Zhenglan Banner. *Geographical Research*, *30*, 1669–1682.

Reynolds, J. F., Smith, D.M. S., Lambin, E. F., Turner, B.L., II, Mortimore, M., Batterbury, S. P. J., et al. (2007). Global desertification: Building a science for dryland development. *Science*, *316*, 847–851.

Rogan, J., Franklin, J., & Roberts, D. A. (2002). A comparison of methods for monitoring multitemporal vegetation change using Thematic Mapper imagery. *Remote Sensing of Environment*, *80*, 143–156.

Rubio, J. L., & Bochet, E. (1998). Desertification indicators as diagnosis criteria for desertification risk assessment in Europe. *Journal of Arid Environments*, *39*, 113–120.

Sharma, K. D. (1998). The hydrological indicators of desertification. *Journal of Arid Environments*, *39*, 121–132.

Somers, B., Asner, G. P., Tits, L., & Coppin, P. (2011). Endmember variability in spectral mixture analysis: A review. *Remote Sensing of Environment*, *115*, 1603–1616.

Sommer, S., Zucca, C., Grainger, A., Cherlet, M., Zougmore, R., Sokona, Y., et al. (2011). Application of indicator systems for monitoring and assessment of desertification from national to global scales. *Land Degradation & Development*, *22*, 184–197.

Symeonakis, E., & Drake, N. (2004). Monitoring desertification and land degradation over sub-Saharan Africa. *International Journal of Remote Sensing*, *25*, 573–592.

Tompkins, S., Mustard, J. F., Pieters, C. M., & Forsyth, D. W. (1997). Optimization of endmembers for spectral mixture analysis. *Remote Sensing of Environment*, *59*, 472–489.

Wan, J., & Yan, J. P. (2012). Analysis on characteristics of climate change in Ningxia in recent 51 years. *Resource Development & Market*, *28*, 511–514.

Wang, J. H., & Sun, S. H. (1996). Classification of desertification types and its quantification evaluation system. *Arid Environmental Monitoring*, *10*, 129–137.

Wang, T., Wu, W., Xue, X., Zhang, W. M., Han, Z. W., & Sun, Q. W. (2004). Spatial–temporal changes of sandy desertified land during last 5 decades in northern China. *Acta Geographica Sinica*, *59*, 203–212.

Wessels, K. J., Prince, S. D., & Reshef, I. (2008). Mapping land degradation by comparison of vegetation production to spatially derived estimates of potential production. *Journal of Arid Environments*, *72*, 1940–1949.

Wessels, K. J., van den Bergh, F., & Scholes, R. J. (2012). Limits to detectability of land degradation by trend analysis of vegetation index data. *Remote Sensing of Environment*, *125*, 10–22.

Xu, L. G., Tang, Y., Du, L., & Bao, Z. Y. (2012). Analysis of multi-time scale variability of available precipitation for 58 years in Ningxia. *Journal of Irrigation and Drainage*, *31*, 85–90.

Yan, C. Z., Wang, Y. M., Feng, Y. S., & Wang, J. H. (2003). Macro-scale survey and dynamic studies of Sandy Land in Ningxia by remote sensing. *Journal of Desert Research*, *23*, 132–135.

Yang, X., & Liu, Z. (2005). Using satellite imagery and GIS for land-use and land-cover change mapping in an estuarine watershed. *International Journal of Remote Sensing*, *26*, 5275–5296.

Yang, J., Weisberg, P. J., & Bristow, N. A. (2012). Landsat remote sensing approaches for monitoring long-term tree cover dynamics in semi-arid woodlands: Comparison of vegetation indices and spectral mixture analysis. *Remote Sensing of Environment*, *119*, 62–71.

Yang, L. H., Wu, J. G., & Shen, P. Y. (2013). Roles of science in institutional changes: The case of desertification control in China. *Environmental Science & Policy*, *27*, 32–54.

Yu, L. M., Wang, Z. P., Jiang, A.D., Ren, J., & Li, Q. B. (2011). Dynamic change trend analysis of Ningxia desertification. *Ningxia Journal of Agriculture and Forestry Science and Technology*, *52*, 54–56.

Zucca, C., Peruta, R. D., Salvia, R., Sommer, S., & Cherlet, M. (2012). Towards a world desertification atlas. Relating and selecting indicators and data sets to represent complex issues. *Ecological Indicators*, *15*, 157–170.